

1 Article

2 Optimization of Time-Weighted Average Air 3 Sampling by Solid-Phase Microextraction Fibers 4 Using Finite Element Analysis Software

5 Bulat Kenesov ^{1,*}, Jacek A. Koziel ², Nassiba Baimatova ¹, Olga P. Demyanenko ¹ and Miras
6 Derbissalin ¹

7 ¹ Al-Farabi Kazakh National University, Center of Physical Chemical Methods of Research and Analysis,
8 Almaty 050012, Kazakhstan; bkenesov@cfhma.kz (B. K.), baimatova@cfhma.kz (N. B.),
9 demyanenko@cfhma.kz (O. D.), derbissalin@cfhma.kz (M. D.)

10 ² Iowa State University, Department of Agricultural and Biosystems Engineering, Ames, IA, 50011, USA;
11 koziel@iastate.edu

12 * Correspondence: bkenesov@cfhma.kz; Tel.: +7-727-2390624

13

14 **Abstract:** Determination of time-weighted average (TWA) concentrations of volatile organic
15 compounds (VOCs) in air using solid-phase microextraction (SPME) is advantageous over other
16 sampling techniques, but is often characterized by insufficient accuracies, particularly at longer
17 sampling times. Experimental investigation of this issue and disclosing the origin of the problem is
18 problematic and often not practically feasible due to high uncertainties. This research is aimed at
19 developing the model of TWA extraction process and optimization of TWA air sampling by SPME
20 using finite element analysis software (COMSOL Multiphysics). It was established that sampling by
21 porous SPME coatings with high affinity to analytes is affected by slow diffusion of analytes inside
22 the coating, an increase of analytes concentrations in the air near the fiber tip due to equilibration,
23 and eventual lower sampling rate. The increase of a fiber retraction depth (Z) resulted in better
24 recoveries. Sampling of studied VOCs using 23-ga Car/PDMS assembly at maximum possible Z (40
25 mm) was proven to provide more accurate results. Alternative sampling configuration based on
26 78.5 × 0.75 mm i.d. SPME liner was proven to provide similar accuracy at improved detection limits.
27 Its modification with the decreased internal diameter from the sampling side should provide even
28 better recoveries. The developed model offers new insight into optimization of air and gas sampling
29 using SPME.

30 **Keywords:** solid-phase microextraction; air sampling; air analysis; volatile organic compounds;
31 COMSOL; time-weighted average.

32

33 1. Introduction

34 Analysis of time-weighted average (TWA) concentrations of volatile organic compounds
35 (VOCs) in ambient and indoor (occupational) air is an important part of environmental monitoring
36 programs aiming at chronic exposure or background concentrations. Such analysis is commonly
37 conducted using gas chromatography (GC) in combination with various sampling and sample
38 preparation approaches. Passive sampling is a common approach for determination of TWA
39 concentrations because of its simplicity and low cost. However, most techniques require additional
40 sample preparation and thermal desorption in a separate unit connected to a GC [1].

41 Solid-phase microextraction (SPME) is the only TWA sampling technique, which does not
42 require additional stages and/or equipment [2]. It is based on sampling via the passive VOCs
43 extraction by a fiber coating retracted inside a protecting needle followed by thermal desorption
44 inside a GC injection port [3,4]. Desorption of VOCs from SPME coating is fast and does not require
45 cryogenic or another type of focusing as is the case with whole air- or sorbent tube-based samples [5].

46 In the TWA mode, the SPME device with retracted fiber is deployed into a sampling location for the
47 desired period (e.g., 24 h for daily average sampling), then isolated from possible interferences during
48 storage and transport to a laboratory and analyzed.

49 Calibration is relatively simple compared with “classic” exposed SPME fiber that is subject to
50 variable thickness of the boundary layer that affects the rate of extraction [6,7]. TWA sampling by
51 retracted SPME fibers is described by the simplified version of the Fick’s law of diffusion [3]:
52

$$\bar{C} = \frac{nZ}{ADt} \quad (1)$$

53
54 where: C – TWA concentration of an analyte; n – amount (mass or number of moles) of analyte
55 extracted by coating; Z – diffusion path length (retraction depth from the needle opening to the tip of
56 the fiber); A – internal cross-section area of a protecting needle; D – gas-phase molecular diffusion
57 coefficient for a VOC; t – sampling time.

58 Eq. (1) can also be interpreted by extraction process, i.e., the amount of analyte extracted is
59 proportional to TWA concentration outside of the SPME needle opening, needle opening area,
60 sampling time, and the gas-phase molecular diffusion coefficient, and inversely proportional to
61 retraction depth.

62 Several important assumptions are made with the application of Eq. (1) to TWA-SPME, i.e., (1)
63 fiber coating acts as a “zero sink” and does not affect the rate of sampling, (2) SPME fiber coating is
64 consistent and reliably responding to changing concentrations in the bulk gas-phase outside of the
65 needle opening, and (3) gas-phase concentration in the bulk are the same as at the face of the fiber
66 needle opening.

67 To date, all published research on TWA-SPME used Eq. (1) as the basis of quantification [3,4,8–
68 17] of VOCs in laboratory air, pyrolysis reactor air, engine exhaust, and process air. Eq. (1) predicted
69 measured gas concentrations with reasonable accuracy and precision. However, more evidence
70 suggests that the discrepancies between the model and experimental data exist. Woolcock et al. [15]
71 reported a significant departure from the zero-sink assumption and from Eq. (1) suggesting
72 ‘apparent’ diffusion coefficient (D) dependent on both sampling time (t) and retraction depth (Z).
73 Baimatova et al. [9] reported significant differences in the extracted mass of naphthalene gas for
74 different SPME coatings, i.e., that Eq. (1) does not incorporate. Recent research by Tursumbayeva [18]
75 shows that the discrepancy between Eq. (1) and experimental data are amplified when a wide-bore
76 glass liner is used for passive sampling with SPME fiber retracted inside it. Work by Tursumbayeva
77 [18] suggests that not only the tip of the fiber coating (at the physical retraction depth Z) is involved
78 in extraction, but the whole fiber coating surface with an ‘apparent’ Z that is ~55% longer. Apparent
79 saturation sorption kinetics might also be involved as predicted by Semenov et al. (2000) [19]. Thus,
80 research is warranted to address apparent problems with the use of Eq. (1).

81 Despite the simplicity, quantification of TWA concentrations of VOCs in ambient air using SPME
82 can be associated with poor accuracy and precision [17]. Possible problems are variability of
83 extraction efficiencies associated with inherent and acquired variability between individual SPME
84 fibers, adsorption of analytes by metallic surfaces [14,17], effects of sampled air temperature and
85 humidity.

86 Experimental optimization of the gas sampling process is very time-consuming, particularly at
87 longer extraction times (>24 h). Such experimental setups are quite complex, difficult to build and
88 properly maintain in steady-state conditions (e.g., without leaks and with minimal impact of sorption
89 onto the system itself). During experiments, the sensitivity of the analytical instrument can change
90 leading to additional uncertainties. Uncertainties during experimental method optimization do not
91 allow studying effects of parameters having potentially minor impacts on accuracy and precision.

92 The numerical simulation could provide useful data at various sampling parameters in much
93 faster and more accurate way. It could also allow modeling the sensitivity of Eq. (1) to ranges of
94 practical (user controlled) parameters for air sampling with retracted SPME. COMSOL Multiphysics
95 allowed efficient numerical modeling of the SPME process using finite element analysis-based model

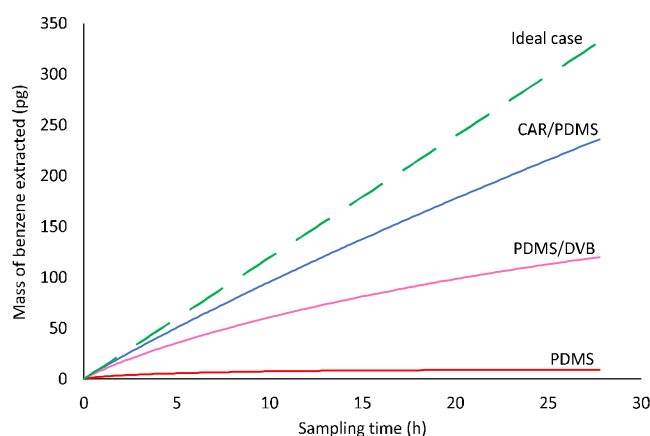
96 [20–25] for liquid-phase extraction and absorption by SPME coating. Using this approach, it was
97 possible to predict sampling profiles of analytes, which were consistent with experimental data.

98 The goal of this research was to develop a model for TWA-SPME and optimize time-weighted
99 average SPME sampling of ambient air with both absorptive and adsorptive retracted fibers using
100 finite element analysis-based model (COMSOL Multiphysics). Specifically, the effects of SPME
101 sampling time, coating type, diffusion coefficient, fiber coating-gas distribution constant, the internal
102 diameter of protecting needle, and SPME retraction depth on extraction were modeled for several
103 common VOCs.

104 2. Results and discussion

105 2.1. TWA sampling profiles of benzene from air using different coatings

106 A sampling of VOCs from the air via retracted SPME has been described using a simplified form
107 of the Fick's first law of diffusion (Eq. 1). However, this equation works only when a SPME fiber acts
108 as a "zero sink" sorbent. Modeling using COMSOL software allowed obtaining sampling profiles for
109 benzene (Figure 1). Closer inspection of Figure 1 illustrates that none of the studied coatings behave
110 as "zero sink" sorbent adhering to Eq. (1), an effect amplified by extended sampling time. After
111 100,000 s of sampling, Car/PDMS, PDMS/DVB, and PDMS extracted 76, 38 and 2.7%, respectively, of
112 the theoretically required for a passive sampling technique. Even if sampling time is decreased to
113 10,000 s, recoveries for these three SPME fiber coatings were 90, 69 and 12.6%, respectively. At
114 sampling time 1000 s, recoveries were 97, 88 and 32% for Car/PDMS, PDMS/DVB and PDMS,
115 respectively.



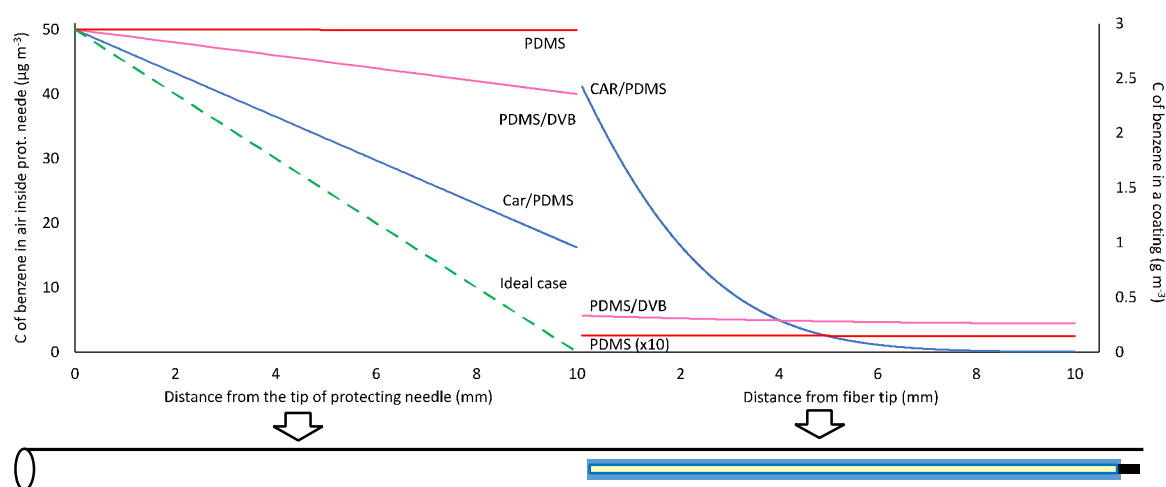
116
117 **Figure 1.** Benzene sampling profiles from ambient air ($T = 298\text{ K}$, $p = 1\text{ atm}$, $C_{\text{benzene}} = 50\text{ }\mu\text{g m}^{-3}$) obtained using
118 different fiber coatings. The ideal case pertains to Eq. (1).
119

120 One feasible explanation for the departure from Eq. (1) is that it can be caused by the increase of
121 the analyte concentration in the air near the fiber tip (Figure 2), which is directly proportional to the
122 analyte concentration in the fiber tip continuously increasing during the sampling. The increase of
123 analyte concentration in the air near the fiber tip results in the decrease of the analyte flux (i.e., the
124 mass of analyte entering protecting needle per cross-sectional area and time) from the sampled air
125 with time. This affects the sampling rate, which was previously assumed to be constant [3,4,8–17].

126 SPME fiber coating can affect the apparent rate of sampling. This was previously assumed to be
127 negligible. According to the Figure 2, Car/PDMS is the most efficient coating for TWA sampling of
128 benzene because it provides the highest benzene extraction effectiveness indicated by the highest
129 distribution constant. However, sampling by this coating is limited by the diffusion of an analyte via
130 pores of the adsorbent (Figure 2). At sampling time 100,000 s, the closest 1 mm of the Car/PDMS
131 coating to the needle opening contains 41% of the total extracted analyte. Benzene concentration in
132 the fiber tip is about 500 times higher than in its other end (furthest from the needle opening). For
133 PDMS/DVB coating, the concentration in the tip is about 24% higher. Slower diffusion of benzene via
134 pores of Car/PDMS fiber is caused by the higher affinity of benzene to the surface of the solid phase

135 (higher distribution constant), and lower porosity. Such ununiform distribution of analytes in the
 136 Car/PDMS may be the reason of their slow desorption after TWA sampling and highly tailing peaks,
 137 particularly for most volatile analytes, which cannot be cold-trapped and refocused in a column front
 138 without cryogenes. This problem also decreases the accuracy of the method.

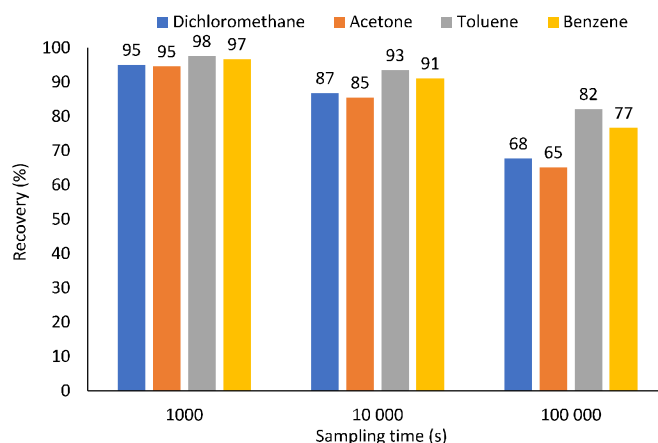
139 The accuracy of the model was validated by increasing the pore diffusion coefficient of benzene
 140 inside Car/PDMS coating by three orders of magnitude. In this case, benzene sampling profile was
 141 the same as predicted by the Eq. (1). This also confirms that an analyte diffusion coefficient inside a
 142 coating affects sampling profiles and accuracy of its quantification using TWA SPME. The model has
 143 also been validated in the 3D mode of COMSOL software, which is much slower compared to 2D.
 144 The difference between the results of 2D and 3D modeling were below 2%, which confirms the
 145 accuracy of the 2D model.



146
 147 **Figure 2.** Concentrations of benzene in different parts of retracted TWA SPME air sampling device at fiber
 148 retraction depth (Z) 10 mm after 100,000 s of sampling.

149 2.2. Effect of the diffusion coefficient and distribution constant on sampling of analytes by CAR/PDMS 150 coating

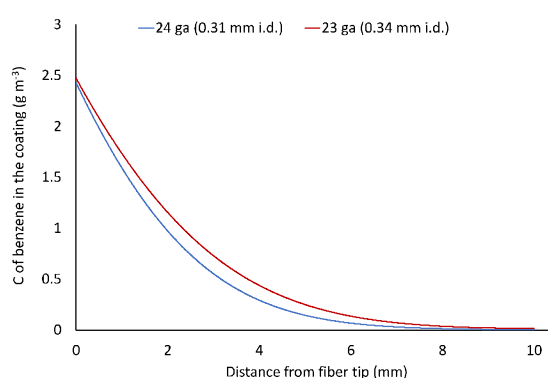
151 The CAR/PDMS coating was used for simulations of extractions for other common VOCs
 152 associated with a wide range of diffusion coefficients and distribution constants. During 100,000 s,
 153 3.3, 3.9, 3.5 and 3.3 pmol of dichloromethane, acetone, toluene, and benzene, respectively, were
 154 extracted, which corresponds to 68, 65, 82 and 77% of the theoretical values predicted by Eq. (1)
 155 (Figure 3). The lowest value was observed for acetone having distribution constant close to
 156 dichloromethane, and the highest diffusion coefficient among studied compounds. Highest recovery
 157 was observed for toluene having the lowest diffusion coefficient and the highest distribution
 158 constant. Thus, both diffusion coefficient and distribution constant affect the recovery of sampled
 159 analytes. Highest recovery can be achieved at the lowest diffusion coefficient and highest distribution
 160 constant. At sampling times 1000 and 10,000 s, recoveries are greater (95-98 and 85-93%, respectively)
 161 and less affected by analyte's properties.



162
163 **Figure 3.** TWA sampling profiles and recoveries of analytes having different diffusion coefficients
164 and distribution constants.

165 2.3. Effect of a protecting needle gauge size

166 Commercial SPME fiber assemblies are available with two different sizes of a protecting needle
167 - 24 and 23 ga having an internal diameter (i.d.) 310 and 340 μm , respectively. A cross-section area of
168 the 23-ga needle is 20.3% greater than that of 24-ga needle, which (according to Eq. 1) should result
169 in the proportionally greater mass of an analyte extracted by a 23-ga SPME assembly. However, as
170 shown above, faster extraction rates result in a faster saturation of the coating and lower recovery at
171 longer sampling times. According to the results of COMSOL simulations, despite ~19% greater
172 masses of extracted analytes compared to a 24-ga assembly, sampling with a 23-ga assembly provided
173 similar greater recoveries of analytes. Such results can be explained by considering the effect of a
174 greater space between a coating and an internal wall of a protecting needle allowing faster diffusion
175 of analytes to the side and rear sides of a coating (Figure 4). This is consistent with recent experimental
176 observations where wide-bore glass liners were used (actual measured I.D. is ~0.84 mm compared
177 with the nominal 0.75 mm I.D.) instead of SPME needle for sampling with retracted fiber [18]. Thus,
178 TWA sampling using 23-ga SPME assembly is recommended over 24-ga for achieving lower
179 detection limits without negative impact on the accuracy. All further modeling was conducted using
180 23-ga SPME device.

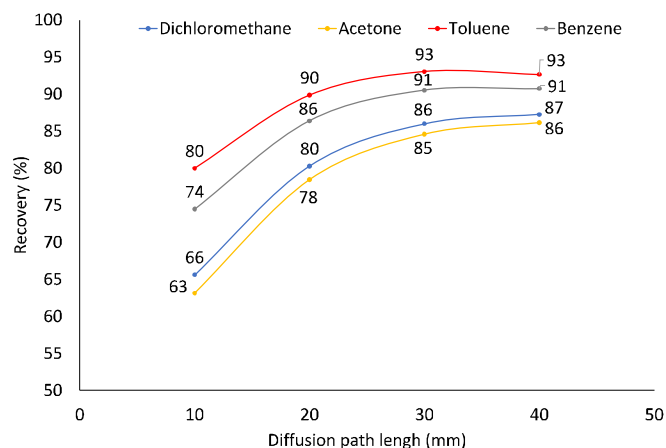


181
182 **Figure 4.** Effect of protecting needle gauge size concentration profile of benzene in the Car/PDMS coating after
183 100,000-s sampling.

184 2.4. Effect of diffusion path (Z) at constant analyte concentration in sampled air

185 Diffusion path length is one of the two parameters that can easily be adjusted by users for
186 achieving the optimal sampling conditions (the other one being sampling time). The increase of Z
187 decreases the rate of sampling. It slows down the saturation of the fiber tip and increases recoveries
188 of analytes (Figure 5) at longer sampling times. For all studied analytes, at $t = 100,000$ s and $Z = 40$
189 mm, recovery was 86-93 % compared to 63-80% at $Z = 10$ mm (Figure 5). The only major drawback of

190 the increase of Z is the decrease of an analyte mass extracted by a coating and a lower analytical
 191 signal, which result in the increased detection limits. At $Z = 40$ mm, $C = 50 \mu\text{g m}^{-3}$ and $t = 100,000$ s,
 192 23-ga Car/PDMS assembly extracts 100 pg of benzene. For GC-MS, the detection limit of benzene is
 193 less than 2 pg [26] meaning that the detection limit will be $\sim 1 \mu\text{g m}^{-3}$, which is five times lower than
 194 the maximum permissible annual average concentration of benzene in ambient air in EU ($5 \mu\text{g m}^{-3}$).
 195 In other countries, permissible concentrations are even higher.
 196

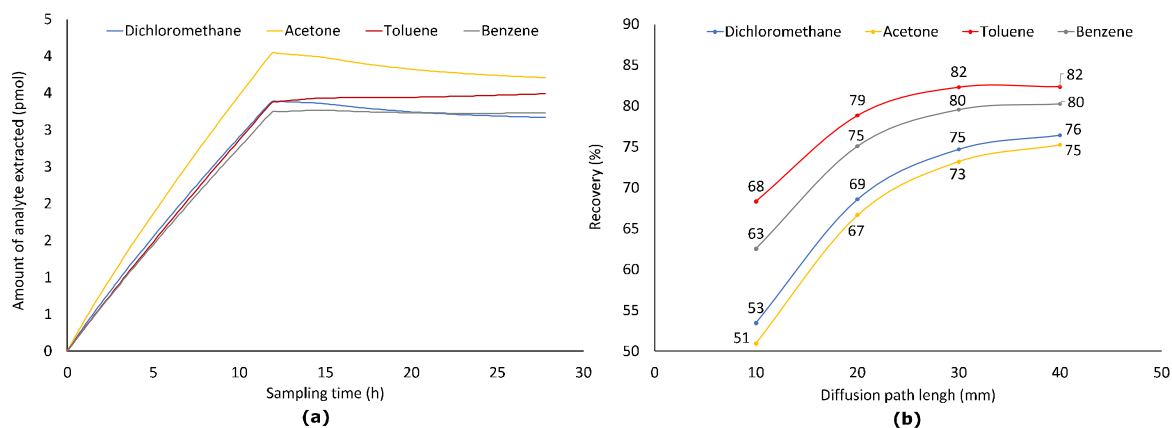


197
 198 **Figure 5.** Effect of diffusion path length on recoveries of four analytes after sampling for 100,000 s using 23-ga
 199 Car/PDMS fiber assembly.

200 2.5. Effect of diffusion path (Z) at variable analyte concentration in sampled air (worst-case scenario)

201 Time-weighted average sampling is conducted during long time periods (e.g., 24 h), during
 202 which concentrations of analytes in the sampled air can significantly vary. The apparent worst-case
 203 scenario can be when in the first half of sampling, concentration is much higher than during the
 204 second half. When the concentration of an analyte in the sampled air becomes close to or lower than
 205 the concentration near the fiber tip, the flux of analytes can go to a reverse direction resulting in
 206 desorption of analytes from a coating. However, it violates the main principle of TWA sampling - the
 207 rate of sampling should depend only on the concentration of an analyte in a sampled air. It means
 208 that if an analyte concentration in sampled air is zero, a rate of extraction should also be equal to zero.
 209 Thus, the aim of this part of the work was to model such a case and estimate the highest possible
 210 uncertainty of the TWA SPME sampling approach.

211 As it was assumed, desorption of dichloromethane, acetone, and benzene from a fiber started
 212 after concentrations of analytes dropped from 91.7 to $9.17 \mu\text{g m}^{-3}$ in the middle of extraction process
 213 (Figure 6). Desorption of toluene was not observed because it has the highest distribution constant
 214 among all studied analytes. However, a sampling of toluene after the drop of its concentration in
 215 sampled air was lower than theoretical. Recoveries of analytes at $Z = 10$ mm dropped from 63-80
 216 to 53-67%, at $Z = 20$ mm – from 78-90 to 67-79%, at $Z = 30$ mm – from 85-93 to 73-82, at $Z = 40$ mm – from
 217 86-93 to 75-82 % (Figure 6). Only at $Z = 40$ mm, it was possible to keep recovery of all analytes above
 218 75%. Thus, if possible, for greater accuracy, sampling must be arranged so that no significant drop in
 219 concentration takes place. Such drop can be observed, e.g., if the end of sampling is planned for the
 220 night when the VOC concentrations in ambient air are typically lower due to much lower road traffic
 221 and other human activities. Also, using shorter sampling times can minimize the risk of reverse
 222 diffusion when ambient concentrations are predicted to drop significantly.

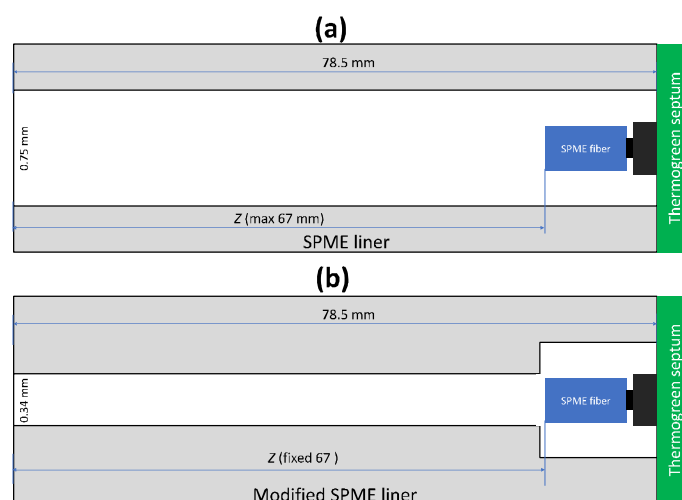


223
224 **Figure 6.** Sampling ($Z = 10$ mm) profiles of four analytes from air having their varying concentrations ($C_{0-49,000\text{ s}} =$
225 $1.176 \mu\text{mol m}^{-3}$, $C_{49,000-51,000\text{ s}} = 1.176 - 0.1176 \mu\text{mol m}^{-3}$, $C_{49,000-100,000\text{ s}} = 0.1176 \mu\text{mol m}^{-3}$) and recoveries of analytes
226 at $t = 100,000\text{ s}$ and different Z .

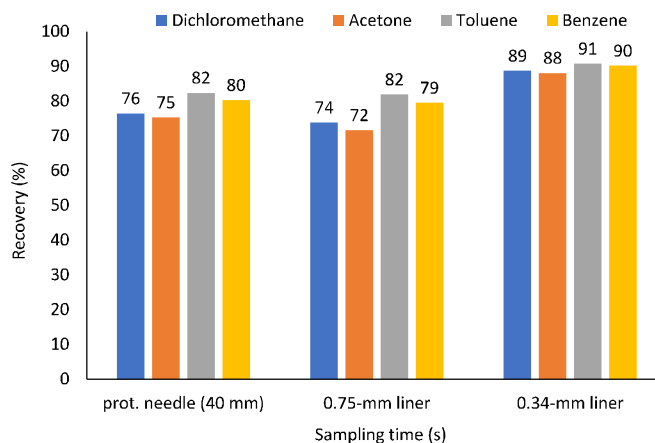
227 2.6. Alternative geometries for TWA SPME sampling

228 As was shown above, an increase of the internal diameter of a protecting needle provides more
229 space for analytes to diffuse around the coating and better reach the side of the coating. It decreases
230 the controlling role of the fiber coating tip and should lead to more accurate and reproducible results.

231 Tursumbayeva [18] proposed using SPME liner for TWA SPME to avoid sorption of analytes
232 onto metallic walls of a protecting needle. The same approach can be used to avoid equilibration of
233 analytes between the fiber tip and surrounding space after sampling over longer time periods. At
234 variable concentrations of analytes (as simulated in the previous section), calculated recoveries for
235 VOCs using $Z = 67$ mm (Figure 7a) are 72-82%, which are close to the values obtained using retracted
236 fiber at $Z = 40$ mm. No improvement was observed because of 0.75-mm i.d. SPME liner has 4.9 times
237 greater cross-sectional area than 23-ga protecting needle, which results in 2.9 times greater theoretical
238 flux of analytes from sampled air to the coating under the set Z (67 and 40 mm, respectively). To
239 decrease the flux of analytes, the liner can be modified to a lower i.d. (e.g., 0.34 mm as for 23-ga
240 needle) from the sampling side almost to the expected location of the fiber as shown in Figure 7b.
241 Under these conditions, recoveries increased to 88-91% (Figure 8).

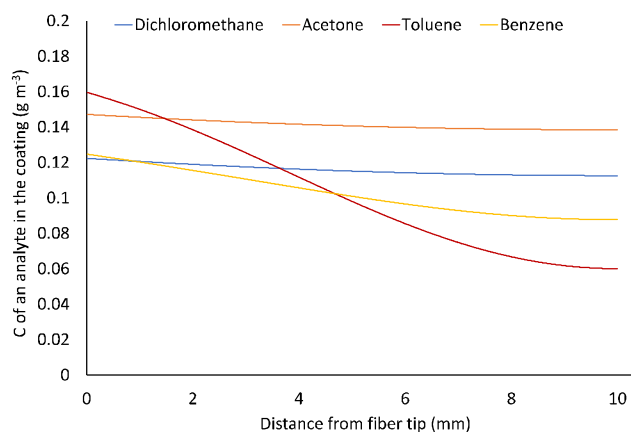


242
243 **Figure 7.** Alternative geometries for TWA SPME sampling: (a) used by Tursumbayeva [18], and (b) proposed in
244 this research to minimize sources of deviation from Fick's law of diffusion calibration



245
246 **Figure 8.** Effect of TWA SPME sampling geometry on recoveries ($t = 100,000$ s, $C_{0-49,000\text{ s}} = 1.176 \mu\text{mol m}^{-3}$, $C_{49,000-51,000\text{ s}} = 1.176 - 0.1176 \mu\text{mol m}^{-3}$, $C_{49,000-100,000\text{ s}} = 0.1176 \mu\text{mol m}^{-3}$)

249 The use of alternative geometries (Figure 9) resulted in a more uniform distribution of the
250 analytes in a coating – for 0.75 mm i.d. SPME liner concentrations of analytes near the fiber tip were
251 only 1.1-2.7 times greater than at another side of the coating. This should result in faster desorption
252 of analytes, less pronounced peak tailing and greater accuracy of the method. The same effect is used
253 when using radiello® passive air sampler [27].



254
255 **Figure 9.** Profiles of analyte concentration in the Car/PDMS coating after sampling ambient air ($C_{0-49,000\text{ s}} = 1.176$
256 $\mu\text{mol m}^{-3}$, $C_{49,000-51,000\text{ s}} = 1.176 - 0.1176 \mu\text{mol m}^{-3}$, $C_{49,000-100,000\text{ s}} = 0.1176 \mu\text{mol m}^{-3}$) for 100,000 s using the geometry
257 presented in Figure 7a.

258 3. Materials and Methods

259 3.1. General parameters of modeling

260 Simulations were completed using COMSOL Multiphysics 5.3a on a desktop computer
261 equipped with quad-core Core i5 processor and 8 Gb of random-access memory. For modeling,
262 “Chemical Species Transport” module (“Transport of diluted species” or “Transport of diluted
263 species in porous media” physics) was used in “Time-Dependent” mode in two dimensions
264 (axisymmetric). Fick’s second law of diffusion was used by the module:

$$265 \frac{\partial c_i}{\partial t} = \nabla \cdot (D_i \nabla c_i) \quad (2)$$

266 Benzene, a ubiquitous air pollutant, was used as a model analyte for most initial calculations.
267 Diffusion coefficients of benzene in the air and PDMS coating were set to $8.8 \cdot 10^{-6}$ and $10^{-10} \text{ m}^2 \text{ s}^{-1}$,
268

269 respectively [28]. Distribution constant (K_d) for benzene and common SPME coatings was set to
 270 150,000 (85 μm Carboxen (Car)/PDMS) [29], 8,300 (65 μm PDMS/DVB) [29], and 301 (PDMS) [5]. For
 271 dichloromethane, acetone and toluene, distribution constants between 85 μm Car/PDMS and air were
 272 set to 72,000, 71,000 and 288,000, respectively [29].

273 The geometry of a fiber assembly was built in as inputs based on Pawliszyn [5]. Simulations
 274 were conducted for Stableflex fibers with a core diameter of 130 μm . For 85 μm Car/PDMS and 65
 275 μm PDMS/DVB, total fiber diameters were set to 290 and 270 μm , respectively. Most calculations
 276 were conducted for 24 ga coating having internal diameter 310 μm .

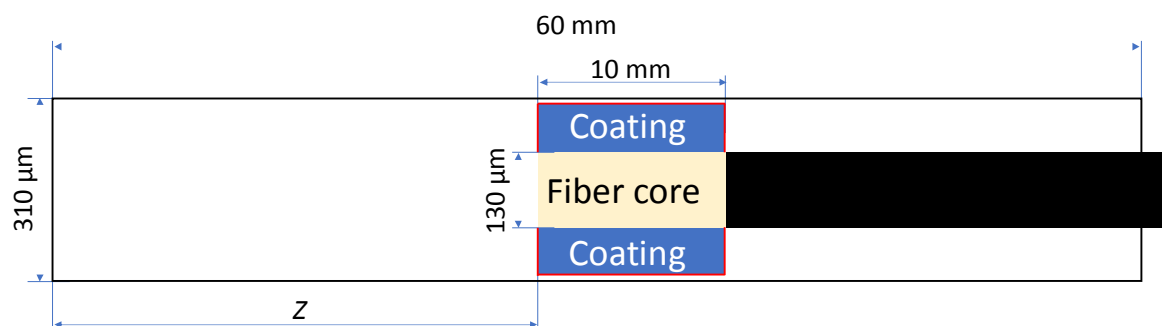
277 The extra fine free triangular mesh was used for the modeling. To provide better meshing at the
 278 coating-air interface, resolution of narrow regions was increased to '2'. The computation was
 279 completed in the range between 0 and 100,000 s at the step of 1,000 s. The concentration of an analyte
 280 at the tip of the protecting needle was set to 6.41E-7 mol m⁻³, which corresponds to 50 $\mu\text{g m}^{-3}$ of
 281 benzene.

282 3.2. Sampling using absorptive coatings

283 Inward (and outward) fluxes from (or backward to) air into an absorptive coating at the
 284 boundary layer (marked by a red line in Figure 10) were simulated using the equation, previously
 285 proposed by Mackay and Leinonen [30] for the water-air interface:

$$286 \text{Flux}_1 = k_1 \cdot \left(C_a - \frac{C_f}{K_d} \right); \quad \text{Flux}_2 = k_2 \cdot \left(\frac{C_f}{K_d} - C_a \right) \quad (3)$$

287 where: k_1 and k_2 – flux coefficients from air to fiber and backward, respectively; C_a and C_f –
 288 concentrations of an analyte in air and coating at the boundary layer, respectively; K_d – distribution
 289 constant for a VOCs between SPME coating and air.
 290



291
 292 **Figure 10.** The geometry of SPME device (retracted inside a protective needle for TWA sampling) used for
 293 modeling. Note: red lines indicate the boundaries between air and coating.
 294

295 True values of flux coefficients were unknown, but in this research, they were assumed to be
 296 sufficiently high for not affecting flux, as was recently proposed by Alam et al. [21]. Thus, flux
 297 coefficient was set to 1,000.

298 3.3. Sampling using adsorptive coatings

299 For adsorptive coatings, "Adsorption" mechanism was activated in the model. Isotropic
 300 diffusion coefficient (in the air inside pores) was the same as for air (set to 8.8, 8.7, 12.4 and 10.1 mm²
 301 s⁻¹ for benzene, toluene, acetone, and dichloromethane, respectively). The approach proposed by
 302 Mocho and Desauziers [31] involving Knudsen diffusion in micro-pores was also tested. However, it
 303 was later rejected for model simplification because the diffusion of analytes inside coating is mainly
 304 driven by molecular diffusion inside macro-pores. The presence of PDMS binder was not considered
 305 in the model because: 1) it has much weaker affinity to analytes than Carboxen; and 2) the layer of
 306 PDMS in the coating is very thin and should not affect the diffusion of analytes [5]; 3) there is not
 307 enough published information about exact structure of the coating.

308 Adsorption was set to “User defined” with a distribution constant (K_p , $\text{m}^3 \text{kg}^{-1}$) calculated as a
309 dimensionless distribution constant divided by a coating density (K_d/ρ). Coating porosities (ϵ) were
310 calculated using intra-particle porosities (0.37 for Car, and 0.55 for DVB [32]) and inter-particle
311 porosity. The exact value of the latter is proprietary and not available in the open literature. Taking
312 into account, the spherical shape of particles and available SEM photos, the inter-particle porosity of
313 both coatings was set to 0.50. A particle porosity (ϵ) was calculated as the total volume of pores (0.78
314 mL for Car, and 1.54 mL for DVB) divided by the total volume of one gram of material (2.13 mL for
315 Car, and 2.78 mL for DVB). Densities of the coatings were calculated using free fall densities of the
316 particles (470 kg m^{-3} for Car, and 360 kg m^{-3} for DVB) [32] and inter-particle porosity. Effective
317 diffusion coefficients were calculated during the calculations by the COMSOL software using the
318 Tortuosity model [31]:
319

$$D_e = \frac{\epsilon D_p}{\tau} \quad (4)$$

320 where: ϵ – porosity; τ – tortuosity calculated from the porosity [31]:
321
322

$$\tau = \epsilon + 1.5(1 - \epsilon) \quad (5)$$

323 For Car/PDMS and PDMS/DVB coatings tortuosity was set to 1.317 and 1.225, respectively.

324 4. Conclusions

325 A finite element analysis-based model (based on COMSOL Multiphysics software) allowed
326 efficient simulation of TWA air sampling of VOCs using retracted SPME fibers. It was possible to
327 model the effects of sampling time, coating type (including adsorptive coatings for the first time) and
328 composition, diffusion coefficient, the distribution constant, the internal diameter of a protecting
329 needle and diffusion path on the recovery of analytes, their concentration profiles in the air inside
330 protecting needle and coating. The advantage of such simulation compared to an experiment are 1)
331 time and cost savings; 2) lower uncertainty and possibility to discover minor impacts of sampling
332 parameters on its performance; and 3) possibility to understand and optimize a sampling process in
333 greater details. All this should lead to lower risk of apparent departure from the Fick’s law of
334 diffusion-based model used for quantification of VOCs with retracted SPME.

335 It was established that sampling by porous coatings with high affinity to the analyte (Car/PDMS)
336 is affected by the saturation of the fiber tip and slow diffusion of analytes in the coating. Highest
337 recoveries are achieved for analytes having lowest diffusion coefficients and highest affinities to a
338 coating. The increase of an internal diameter of a protecting needle from 24 to 23 ga allows obtaining
339 proportionally greater responses at similar recoveries.

340 The most important parameter of a sampling process that users can control is a retraction depth.
341 The increase of Z allows slowing down the sampling and achieving higher recoveries of analytes. In
342 this study, at $Z = 40 \text{ mm}$ and constant analyte concentration in a sampled air, recoveries of studied
343 analytes reached 86-93% compared to 63-80% at $Z = 10 \text{ mm}$. The developed model allowed simulation
344 of the worst sampling case when analytes concentrations significantly drop in the middle of
345 sampling. At $Z = 40 \text{ mm}$, recoveries of analytes dropped by $\sim 10\%$, while at $Z = 10 \text{ mm}$ – by $\sim 15\%$.

346 According to the results of the simulation, it is optimal to conduct sampling of studied VOCs
347 using 23 ga Car/PDMS assembly at $Z = 40 \text{ mm}$. Expected detection limits at these parameters are
348 about $1 \mu\text{g m}^{-3}$.

349 Alternative geometries of a protective TWA SPME sampling devices could be used to increase
350 recoveries of analytes. Sampling using 0.75 mm i.d. SPME GC liner at $Z = 67 \text{ mm}$ provides similar %
351 recoveries compared to sampling using protecting needle at $Z = 40 \text{ mm}$, but it provides greater masses
352 of analytes extracted and lower detection limits. To achieve greater recovery, part of the liner should
353 have narrower i.d. (e.g., 0.34 mm). The increase of the diameter of the extraction zone where the
354 coating is located results in a more uniform distribution of analytes, which should lead to faster

355 desorption, less pronounced peak tailing and greater accuracy. Specific sampler parameters should
356 be selected for particular sampling time and environmental conditions (temperature and atmospheric
357 pressure) using the developed model.

358 The methodology used in this study could also be used for more accurate and simpler calibration
359 of the method. It can be used to model sampling of other environments (process gases, water) by
360 retracted SPME fibers. Further modification of this model could allow simulation of soil and soil gas
361 sampling.

362 **Supplementary Materials:** None.

363 **Author Contributions:** B.K. and J.K. developed the model and designed computational experiments, N.B. and
364 O.D. made the literature review and validated the model, B.K. and M.D. conducted the modeling and processed
365 the data, B.K. and J.K. described the results, B.K., N.B. and O.D. prepared the manuscript for submission. All
366 authors have approved the final version of the manuscript.

367 **Notes:** The authors declare no competing financial interest.

368 **Funding:** This research was funded by the Ministry of Education and Science of the Republic of Kazakhstan,
369 grant number AP05133158. This research was partially supported by the Iowa Agriculture and Home Economics
370 Experiment Station, Ames, Iowa. Project No. IOW05400 (Animal Production Systems: Synthesis of Methods to
371 Determine Triple Bottom Line Sustainability from Findings of Reductionist Research) is sponsored by Hatch Act
372 and State of Iowa funds.

373 **Acknowledgments:** Authors would like to thank the Ministry of Education and Science of the Republic of
374 Kazakhstan for supporting Miras Derbissalin and Olga Demyanenko with Ph.D. and M.S. scholarships,
375 respectively.

376 **Conflicts of Interest:** The authors declare no conflict of interest.

377 **References**

- 378 1. Pienaar, J. J.; Beukes, J. P.; Van Zyl, P. G.; Lehmann, C. M. B.; Aherne, J. Passive diffusion sampling
379 devices for monitoring ambient air concentrations. In *Comprehensive Analytical Chemistry*; Elsevier, 2015;
380 Vol. 70, pp. 13–52 ISBN 9780444635532.
- 381 2. Grandy, J.; Asl-Hariri, S.; Pawliszyn, J. *Novel and Emerging Air-Sampling Devices*; Elsevier, 2015; Vol. 70;
382 ISBN 9780444635532.
- 383 3. Martos, P. A.; Pawliszyn, J. Time-weighted average sampling with solid-phase microextraction device:
384 Implications for enhanced personal exposure monitoring to airborne pollutants. *Anal. Chem.* **1999**, *71*,
385 1513–1520, doi:10.1021/ac981028k.
- 386 4. Khaled, A.; Pawliszyn, J. Time-weighted average sampling of volatile and semi-volatile airborne organic
387 compounds by the solid-phase microextraction device. *J. Chromatogr. A* **2000**, *892*, 455–467,
388 doi:10.1016/S0021-9673(00)00295-8.
- 389 5. Pawliszyn, J. *Handbook of Solid Phase Microextraction*; First Edit.; Elsevier Inc, 2012; ISBN 9780124160170.
- 390 6. Koziel, J.; Jia, M.; Pawliszyn, J. Air sampling with porous solid-phase microextraction fibers. *Anal. Chem.*
391 **2000**, *72*, 5178–5186, doi:10.1021/ac000518l.
- 392 7. Augusto, F.; Koziel, J.; Pawliszyn, J. Design and validation of portable SPME-devices for rapid field air.
393 *Anal. Chem.* **2001**, *73*, 481–486.
- 394 8. Koziel, J. A.; Nguyen, L. T.; Glanville, T. D.; Ahn, H.; Frana, T. S.; (Hans) van Leeuwen, J. Method for
395 sampling and analysis of volatile biomarkers in process gas from aerobic digestion of poultry carcasses
396 using time-weighted average SPME and GC-MS. *Food Chem.* **2017**, *232*, 799–807,
397 doi:10.1016/j.foodchem.2017.04.062.
- 398 9. Baimatova, N.; Koziel, J.; Kenessov, B. Passive sampling and analysis of naphthalene in internal
399 combustion engine exhaust with retracted SPME device and GC-MS. *Atmosphere (Basel)*. **2017**, *8*, 130,
400 doi:10.3390/atmos8070130.
- 401 10. Koziel, J.; Jia, M.; Khaled, A.; Noah, J.; Pawliszyn, J. Field air analysis with SPME device. *Anal. Chim.*
402 *Acta* **1999**, *400*, 153–162, doi:10.1016/S0003-2670(99)00614-5.
- 403 11. Koziel, J. A.; Pawliszyn, J. Air sampling and analysis of volatile organic compounds with solid phase
404 microextraction. *J. Air Waste Manag. Assoc.* **2001**, *51*, 173–184, doi:10.1080/10473289.2001.10464263.
- 405 12. Koziel, J. A.; Noah, J.; Pawliszyn, J. Field sampling and determination of formaldehyde in indoor air
406 with solid-phase microextraction and on-fiber derivatization. *Environ. Sci. Technol.* **2001**, *35*, 1481–1486.
- 407 13. Chen, Y.; Pawliszyn, J. Time-weighted average passive sampling with a Solid-Phase Microextraction
408 device. *Anal. Chem.* **2003**, *75*, 2004–2010, doi:10.1021/ac026315+.
- 409 14. Chen, Y.; Pawliszyn, J. Solid-phase microextraction field sampler. *Anal. Chem.* **2004**, *76*, 6823–8,
410 doi:10.1021/ac0490806.
- 411 15. Woolcock, P. J.; Koziel, J. A.; Cai, L.; Johnston, P. A.; Brown, R. C. Analysis of trace contaminants in hot
412 gas streams using time-weighted average solid-phase microextraction: proof of concept. *J. Chromatogr.*
413 *A* **2013**, *1281*, 1–8, doi:10.1016/j.chroma.2013.01.036.
- 414 16. Woolcock, P. J.; Koziel, J. A.; Johnston, P. A.; Brown, R. C.; Broer, K. M. Analysis of trace contaminants
415 in hot gas streams using time-weighted average solid-phase microextraction: Pilot-scale validation. *Fuel*
416 **2015**, *153*, 552–558, doi:10.1016/j.fuel.2015.02.101.
- 417 17. Baimatova, N.; Koziel, J. A.; Kenessov, B. Quantification of benzene, toluene, ethylbenzene and o-xylene
418 in internal combustion engine exhaust with time-weighted average solid phase microextraction and gas
419 chromatography mass spectrometry. *Anal. Chim. Acta* **2015**, *873*, 38–50, doi:10.1016/j.aca.2015.02.062.

- 420 18. Tursumbayeva, M. *Simple and accurate quantification of odorous volatile organic compounds in air with solid*
421 *phase microextraction and gas chromatography - mass spectrometry*. M.S. thesis; Iowa State University: Ames,
422 Iowa, USA, 2017;
- 423 19. Semenov, S. N.; Koziel, J. A.; Pawliszyn, J. Kinetics of solid-phase extraction and solid-phase
424 microextraction in thin adsorbent layer with saturation sorption isotherm. *J. Chromatogr. A* **2000**, *873*, 39–
425 51, doi:10.1016/S0021-9673(99)01338-2.
- 426 20. Zhao, W. *Solid phase microextraction in aqueous sample analysis*. PhD thesis; 2008; ISBN 9780494433942.
- 427 21. Alam, M. N.; Ricardez-Sandoval, L.; Pawliszyn, J. Numerical modeling of solid-phase microextraction:
428 binding matrix effect on equilibrium time. *Anal. Chem.* **2015**, *87*, 9846–9854,
429 doi:10.1021/acs.analchem.5b02239.
- 430 22. Alam, M. N.; Ricardez-Sandoval, L.; Pawliszyn, J. Calibrant free sampling and enrichment with solid
431 phase microextraction: computational simulation and experimental verification. *Ind. Eng. Chem. Res.*
432 **2017**, *56*, 3679–3686, doi:10.1021/acs.iecr.7b00131.
- 433 23. Souza-Silva, E. A.; Gionfriddo, E.; Alam, M. N.; Pawliszyn, J. Insights into the effect of the PDMS-layer
434 on the kinetics and thermodynamics of analyte sorption onto the matrix-compatible SPME coating. *Anal.*
435 *Chem.* **2017**, *89*, 2978–2985, doi:10.1021/acs.analchem.6b04442.
- 436 24. Alam, M. N.; Pawliszyn, J. Numerical simulation and experimental validation of calibrant-loaded
437 extraction phase standardization approach. *Anal. Chem.* **2016**, *88*, 8632–8639,
438 doi:10.1021/acs.analchem.6b01802.
- 439 25. Alam, M. N.; Nazdrajić, E.; Singh, V.; Tascon, M.; Pawliszyn, J. Effect of transport parameters and device
440 geometry on extraction kinetics and efficiency in direct immersion solid-phase microextraction. *Anal.*
441 *Chem.* **2018**, *in press*, acs.analchem.8b02855, doi:10.1021/acs.analchem.8b02855.
- 442 26. Baimatova, N.; Kenessov, B.; Koziel, J. a.; Carlsen, L.; Bektassov, M.; Demyanenko, O. P. Simple and
443 accurate quantification of BTEX in ambient air by SPME and GC–MS. *Talanta* **2016**, *154*, 46–52,
444 doi:10.1016/j.talanta.2016.03.050.
- 445 27. Boaretto C., Sacco P., C. V. High uptake rate radial diffusive sampler suitable for both solvent and
446 thermal desorption. *Ind. Hyg. Assoc.* **1996**, *57*, 897–904.
- 447 28. Chao, K.-P.; Wang, V.-S.; Yang, H.-W.; Wang, C.-I. Estimation of effective diffusion coefficients for
448 benzene and toluene in PDMS for direct solid phase microextraction. *Polym. Test.* **2011**, *30*, 501–508,
449 doi:10.1016/j.polymertesting.2011.04.004.
- 450 29. Prikryl, P.; Sevcik, J. G. K. Characterization of sorption mechanisms of solid-phase microextraction with
451 volatile organic compounds in air samples using a linear solvation energy relationship approach. *J.*
452 *Chromatogr. A* **2008**, *1179*, 24–32, doi:10.1016/j.chroma.2007.10.016.
- 453 30. Mackay, D.; Leinonen, P. J. Rate of evaporation of low-solubility contaminants from water bodies to
454 atmosphere. *Environ. Sci. Technol.* **1975**, *9*, 1178–1180, doi:10.1021/es60111a012.
- 455 31. Mocho, P.; Desauziers, V. Static SPME sampling of VOCs emitted from indoor building materials:
456 Prediction of calibration curves of single compounds for two different emission cells. *Anal. Bioanal. Chem.*
457 **2011**, *400*, 859–870, doi:10.1007/s00216-011-4820-y.
- 458 32. Tuduri, L.; Desauziers, V.; Fanlo, J. L. Potential of solid-phase microextraction fibers for the analysis of
459 volatile organic compounds in air. *J. Chromatogr. Sci.* **2001**, *39*, 521–529, doi:10.1093/chromsci/39.12.521.
- 460

461 **Sample Availability:** Samples of the compounds are not available from the authors.

462